Interactions between DNA Polymerase β and the Major Covalent Adduct of the Carcinogen (+)-*anti*-Benzo[*a*]pyrene Diol Epoxide with DNA at a Primer−Template Junction†

Suresh B. Singh,‡ William A. Beard,§ Brian E. Hingerty,|| Samuel H. Wilson,§ and Suse Broyde*,⊥

Merck Research Laboratories, P.O. Box 2000, RY50SW-100, Rahway, New Jersey 07065, Laboratory of Structural Biology, NIEHS, Research Triangle Park, North Carolina 27709, Life Sciences Division, Oak Ridge National Laboratory, Oak Ridge, Tennessee 37831, and Department of Biology, New York University, New York, New York 10003-5181

Received August 20, 1997; Revised Manuscript Received November 5, 1997⊗

ABSTRACT: A molecular dynamics simulation has been carried out with DNA polymerase β (β pol) complexed with a DNA primer−template. The templating guanine at the polymerase active site was covalently modified by the carcinogenic metabolite of benzo[*a*]pyrene, (+)-*anti*-benzo[*a*]pyrene diol epoxide, to form the major (+)-*trans*-*anti*-benzo[*a*]pyrene diol epoxide covalent adduct. Thus, the benzo[*a*]pyrenyl moiety (BP) is situated in the single-stranded template at the junction between double- and single-stranded DNA. The starting structure was based on the X-ray crystal structure of the rat β pol primer−template and ddCTP complex [Pelletier, H., Sawaya, M. R., Kumar, A., Wilson, S. H., and Kraut, J. (1994) *Science 264*, 1891−1903]. During the simulation, the BP and its attached templating guanine rearrange to form a structure in which the BP is closer to parallel with the adjacent base pair. In addition, the templating attached guanine is displaced toward the major groove side and access to its Watson−Crick edge is partly obstructed. This structure is stabilized, in part, by new hydrogen bonds between the BP and β pol Asn^{279} and Arg^{283}. These residues are within hydrogen bonding distance to the incoming ddCTP and templating guanine, respectively, in the crystal structure of the β pol ternary complex. Site-directed mutagenesis has confirmed their role in dNTP binding, discrimination, and catalytic efficiency [Beard, W. A., Osheroff, W. P., Prasad, R., Sawaya, M. R., Jaju, M., Wood, T. G., Kraut, J., Kunkel, T. A., and Wilson, S. H. (1996) *J. Biol. Chem. 271*, 12141−12144]. The predominant biological effect of the BP is DNA polymerase blockage. Consistent with this biological effect, the computed structure suggests the possibility that the BP's main deleterious impact on DNA synthesis might result at least in part from its specific interactions with key polymerase side chains. Moreover, relatively modest movement of BP and its attached guanine, with some concomitant enzyme motion, is necessary to relieve the obstruction and permit the observed rare incorporation of a dATP opposite the guanine lesion.

DNA polymerase β (pol β) of vertebrates is believed to play a key role in gap-filling DNA repair synthesis (*1*−*6*) and has been suggested to play a role in replication (*7*−*9*). Because of its small size (39 kDa), it is a convenient model for studying polymerase enzymological properties, such as nucleotidyl transferase, processivity, and fidelity (*10*). A nucleotidyl transfer mechanism has been proposed on the basis of a crystal structure of a rat pol β ternary complex, containing the polymerase together with a DNA primer−template and nonreactive ddCTP as the incoming nucleoside triphosphate (*11*). Recent crystal structures of human DNA polymerase β complexed with blunt-end DNA have offered further insights into the catalytic mechanism (*12*). The human and rat enzymes are 96% identical with the differences confined to the surface of the protein. The majority of these differences are conservative replacements making these enzymes kinetically indistinguishable (W. A. Beard et al., unpublished data). Importantly, it has recently been demonstrated that a single residue, Arg^{283}, which is within hydrogen bonding distance to the templating base, plays a key role in polymerase fidelity and efficient catalysis (*13*).

Benzo[*a*]pyrene is a polycyclic aromatic hydrocarbon precursor present widely in the environment, in automobile exhaust and tobacco smoke, and as a contaminant in foods such as vegetable oils (*14*−*16*). It is metabolically activated to reactive diol epoxide derivatives, including (+)-*anti*-benzo[*a*]pyrene diol epoxide [(7*R*,8*S*)-dihydroxy-(9*S*,10*R*)-epoxy-7,8,9,10-tetrahydrobenzo[*a*]pyrene], which is the only activation product shown to be tumorigenic in animal studies (*17*, *18*). This diol epoxide forms a major (~90%) covalent

† This research is supported by NIH Grants CA-28038 and RR-06458 and Department of Energy Contract DOE-FG02-90ER60931 to S.B. Computations were carried out on a Silicon Graphics Challenge XL computer at Wyeth Ayerst Research, at the National Science Foundation San Diego Supercomputer Center, and at the Department of Energy National Energy Research Supercomputer Center. We thank Professors Nicholas E. Geacintov and Robert Shapiro of the Chemistry Department at New York University for very helpful discussions.

* Corresponding Author. Phone: (212) 998-8231. Fax: (212) 995-4015. E-mail: broyde@nyu.edu.

‡ Merck Research Laboratories.

§ NIEHS.

|| Oak Ridge National Laboratory.

⊥ New York University.

⊗ Abstract published in *Advance ACS Abstracts,* December 15, 1997.

S0006-2960(97)02063-1 CCC: $15.00
Published on Web 01/03/1998

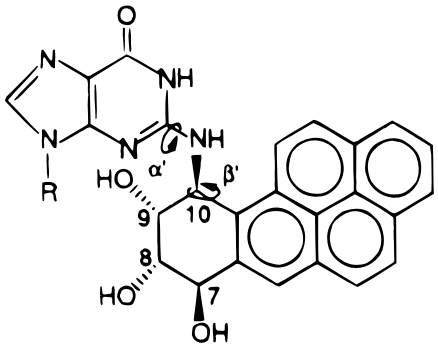

10*S* (+)-*trans-anti*-[BP]-N^2-dG

FIGURE 1: Structure of the (+)-*trans-anti*-[BP]-N^2-dG adduct. The torsion angles α′ and β′, governing the orientation of the BP moiety with respect to the DNA, are indicated by arrows and defined as follows: α′, N1−C2−N^2−[BP]C10; and β′, C2−N^2−[BP]C10−[BP]−C9. The glycosidic torsion angle χ, governing the orientation of the guanine with respect to its sugar, is defined as O4′−C1′−N9−C4. R designates the sugar and the rest of the DNA.

reaction product with DNA at the N^2 of guanine, known as the (+)-*trans-anti*-BP-N^2-dG adduct (*19*−*23*) (Figure 1). It has recently been shown that (racemic) *anti*-benzo[*a*]pyrene diol epoxide reacts preferentially at mutational hot spots of the p53 gene (*24*), which is mutated in many human cancers (*25*). This suggested a causal connection between the major adduct of the tumorigenic diol epoxide and carcinogenesis in humans. A recent comprehensive review summarizes structural and biological work on polycyclic aromatic carcinogen−DNA adducts (*26*).

Computer modeling studies (*27*) had proposed that the benzo[*a*]pyrenyl moiety could reside in the B-DNA minor groove, oriented in the 5′-direction of the modified strand; a structure in which the BP is intercalated into the helix by displacement of the modified guanine into the major groove, with the BP benzylic ring situated on the major groove side of the helix cylinder, and the distal aromatic ring on the opposite, minor groove side, was also computed. High-resolution NMR studies in solution, but without polymerase, have independently demonstrated that these two structural types are observed, in different sequence contexts. In a normal duplex, with equal numbers of residues on the two strands, the minor groove structure is observed (*28*), whereas the base displaced-intercalated structure is observed in a duplex in which the partner to the BP-adducted guanine is missing (*29*). The latter structure is analogous to one in which the replication machinery had skipped the damaged base. Furthermore, when the BP lesion is positioned at a single strand−double strand junction that mimics a primer−template, high-resolution solution NMR studies reveal a related structure where the unpartnered, damaged guanine is displaced from its stacked position, and the BP is now stacked with the base pair 3′ to the adducted guanine (*30*).

To better understand the effects of the (+)-*trans-anti*-BP-N^2-dG lesion on DNA replication, it is necessary to elucidate its conformational features and interactions at a primer−template junction in the presence of a DNA polymerase. At present, there are no crystal structures of any BP-modified DNA available, even in the absence of a polymerase. Moreover, high-resolution NMR is not yet feasible for the large system involving both a full DNA polymerase and BP-modified DNA, although this technique has successfully elucidated the solution structures of BP-modified DNA alone (reviewed in ref *26*). Therefore, to investigate this system, we have carried out a molecular dynamics simulation of the primer−template complex occurring in the rat DNA polymerase β crystal structure (*11*), modified at G4 with the (+)-*trans-anti*-BP-N^2-dG adduct, together with pol β.

5′-d(A1 - A2 - A3 - G4 - G5 - G6 - C7 - G8 - C9 -C10-G11)
d(C18-C17-G16-C15-G14-G13-C12)-5′

This system was chosen to provide the necessary starting coordinates because it was the only available crystal structure of a DNA polymerase containing a primer−template situated at the polymerase active site. The incoming ddCTP was removed from the structure to make room for the BP. The starting orientation of the BP moiety was one that minimized steric close contacts with the enzyme, which placed the BP at a sharp angle to the G5·C18 base pair. During the dynamics simulation, the enzyme, modified G4, and BP moiety rearranged so that G4 was partly displaced from its stacked position with G5, and the BP plane became nearly parallel with the G5·C18 base pair. This structure was stabilized in part by new hydrogen bonds formed with the polymerase, including one between O8 of the BP benzylic ring and an Arg^{283} guanidinium nitrogen. The structure has features consistent with polymerase blockage, the predominant effect of this lesion on DNA replication (*31*−*37*). Furthermore, with modest movement of the BP and G4 from this position and concomitant enzyme motion, an incoming dNTP could be accommodated to overcome the replication block, as observed infrequently in these replication studies.

MATERIALS AND METHODS

The 2.9 Å resolution X-ray crystal structure of rat DNA polymerase β complexed with primer−template (*11*) served as the starting structure. The template and primer sequences were 5′-d(A1-A2-A3-G4-G5-G6-C7-G8-C9-C10-G11) and d(C18-C17-G16-C15-G14-G13-C12)-5′, respectively. In the crystal structure, C18 (i.e. the 3′-terminal primer nucleoside) was a dideoxy derivative, but a deoxy residue was used in the simulation.

Residues 1−8 and 246−248 of the polymerase, as well as the d(A1-A2-A3) residues of the DNA template (i.e. single-stranded overhang), were disordered in the crystal structure, and coordinates were not available. While residues 1−8 of the polymerase are distant from the DNA binding site (more than 28 Å and therefore out of range of the animation, see below), residues 246−248 (Asp, Glu, and Asn) are within the animation range, as are d(A1-A2-A3). Therefore, starting coordinates for these residues were obtained by modeling.

The program QUANTA from Molecular Simulations, Inc., was used to model residues 246−248 in the β strand conformation consistent with the local antiparallel β sheet structure in the vicinity of these residues, and the d(A1-A2-A3) residues were modeled in the B-DNA conformation using the program INSIGHT from Molecular Simulations, Inc. QUANTA and INSIGHT standard values for β strand and B-DNA conformations were employed in this modeling using the QUANTA Karplus rotamer library (*38*) to set the

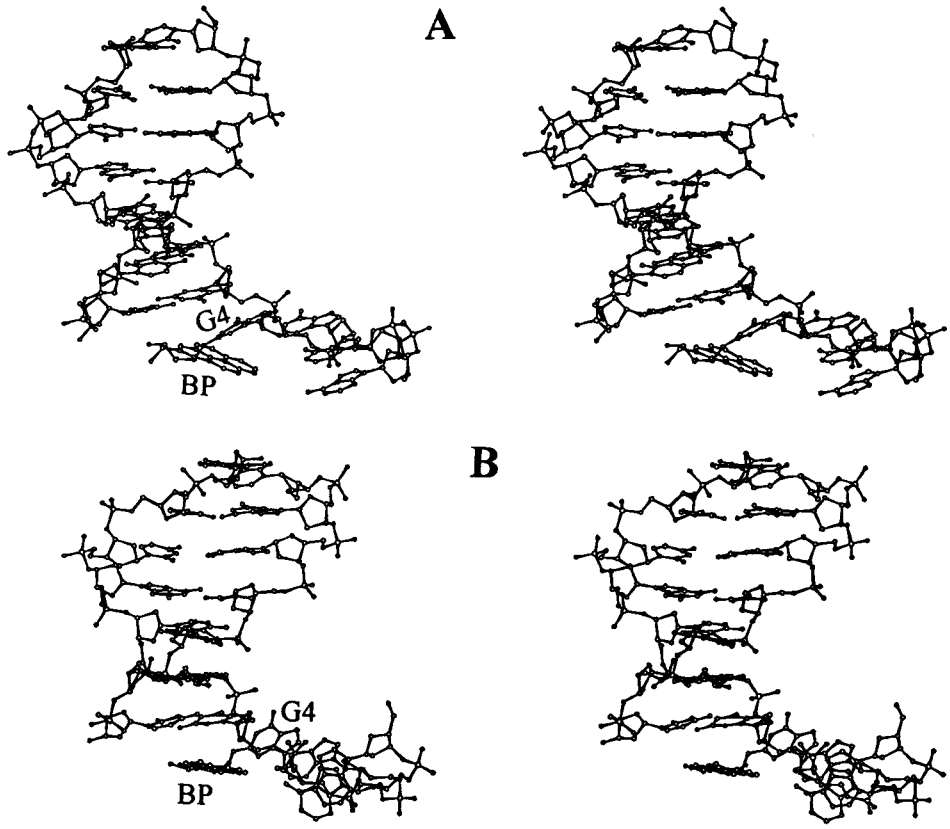

FIGURE 2: Stereoviews of (A) the starting structure and (B) the structure at 200 ps. Hydrogens are omitted for clarity.

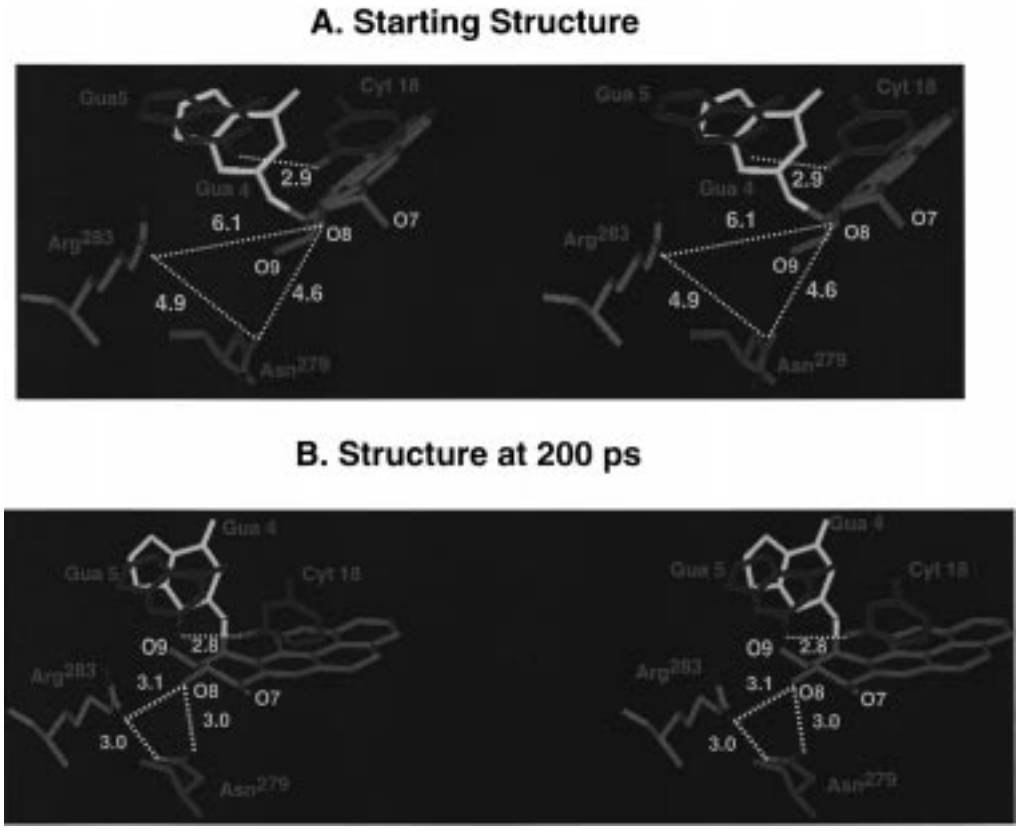

FIGURE 3: Stereoviews of key hydrogen bonding interactions in (A) the starting structure and (B) the structure at 200 ps. Additional hydrogen bonds are given in Table 1, but are omitted here for clarity. The G5·C18 hydrogen bond between G-amino and C-carbonyl is also indicated. Hydrogens are omitted for clarity.

side chain conformations of the amino acids. The B-DNA conformation is that of the fiber diffraction model of Arnott and Hukins (*39*). The ϕ and ψ torsion angles of the modeled β strand conformations are -139 and 135°, respectively.

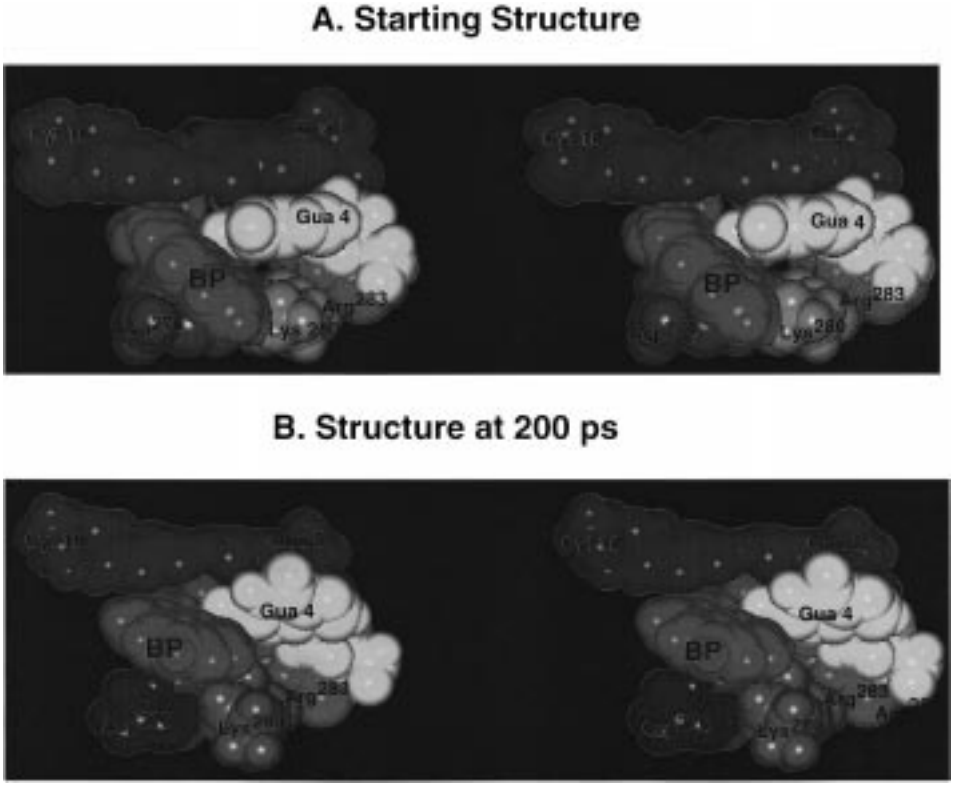

FIGURE 4: Space filling stereoviews of (A) the starting structure and (B) the structure at 200 ps. Bases together with their attached sugars are shown. Hydrogens are omitted for clarity.

The (+)-*trans-anti* BP templating base was constructed by replacing G4 with the modified G taken from our previously computed minor groove structure of this adduct (*27*), but the guanine and the BP were reoriented to minimize collisions with the enzyme. Torsion angles α', β', and χ governing the BP−DNA orientation were 321.1, 266.3, and 253.0°, respectively. This placed the BP along the Watson−Crick edge of G4, the "active" templating base. The ddCTP and its two associated Mg^{2+} ions present in the crystal structure were removed to make room for the BP. Since the DNA phosphates are surrounded by positive charge—protein residues (Arg^{112}, Arg^{137}, Arg^{258}, Arg^{283}, Arg^{299}, Lys^{113}, Lys^{131}, Lys^{230}, and Lys^{234}), polar residues (His^{134}, His^{212}, and Tyr^{296}), and backbone amide nitrogens (Gly^{105}, Gly^{107}, Pro^{108}, Ser^{109}, Lys^{230}, Gly^{232}, Thr^{233}, and Lys^{234})—it was not appropriate to surround the DNA backbone with positively charged counterions.

Minimization and molecular dynamics were carried out with AMBER 4.0 (*40*). [The work was initiated before release of AMBER 4.1 (*41*).] Force field parameters for the BP adduct added to AMBER 4.0 were taken from earlier work (*27*). Successive minimizations consisting of 40 steps of steepest descent followed by 460 steps of conjugate gradient minimization were employed to minimize (1) the positions of the hydrogens which had been added by modeling, keeping the rest of the atoms fixed; (2) the modeled portion of the protein and DNA (these steps were performed prior to replacement of G4 with its BP-modified analogue), and (3) only the BP-modified G4. The BP-modified G4 was then subjected to 2 ps of molecular dynamics at 100 K with a 2.0 fs time step, while the rest of the system was held fixed. The previous steps were carried out in vacuo.

The resulting structure was then solvated with a spherical cap of 2163 TIP3P water molecules (*42*) centered around the BP-modified guanine with a 30 Å radius. The waters were first minimized with 1000 steps of conjugate gradient minimization in which the protein and DNA residues were held by a 25 kcal/mol harmonic restraint. Then, the entire solvated system was minimized with 1000 steps of conjugate gradient minimization, followed by 100 steps of conjugate gradient minimization with covalent bonds to hydrogen fixed with SHAKE (*43*). The solvated system was then heated to 300 K with a temperature coupling constant of 0.2 ps.

Molecular dynamics was carried out with stochastic boundary conditions (*44*); animation was performed for all atoms within a sphere whose minimum radius was 28 Å from any atom in the BP-modified G4 residue. This radius varied between 28 and 35 Å during the simulation, as the algorithm permitted dynamics to the end of any amino acid residue that fell within the 28 Å radius. The static protein residues and solvent molecules were held in their minimized conformation. Of the 12 249 atoms in the system, the 9618 inner ones relative to the BP-modified G4 residue were mobile. A 12 Å uniform cutoff radius was employed for evaluating the nonbonded interactions. Covalent bonds to hydrogen were fixed with SHAKE (*43*). A time step of 2.0 fs was employed. The simulation was carried out for 225 ps.

RESULTS AND DISCUSSION

A rearrangement of the position of the BP moiety from its starting position (Figures 2A, 3A, and 4A) began in the very initial phase of the simulation, during minimization and heating, and was complete by about 16 ps. In this transition, the BP moiety moved to a position where it is closer to parallel with the G5·C18 pair and somewhat stacked with

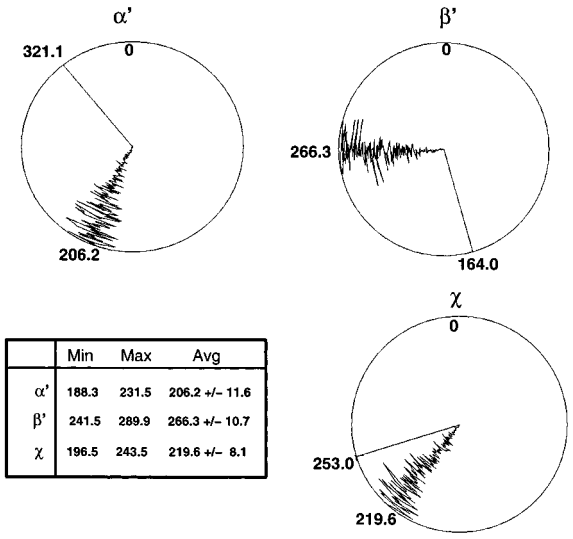

FIGURE 5: Mobility of BP moiety and modified G4 as manifested in torsion angle dynamics of α', β', and χ in degrees. The radius of the circle is the time axis with 0 ps at the center and 200 ps at the circumference. Values for the starting structure are designated with nonfluctuating radii. The inset table gives average values for each quantity together with standard deviations and ranges.

it, while stacking of G4 with G5 is diminished and G4 is displaced. In this position, the BP partly obstructs access to the hydrogen bonding edge of G4, as well as that of the neighboring A3. The structure remains in this position for the duration of the simulation. Figures 2B, 3B, and 4B show the structure at 200 ps. This structure shares features of base displacement and carcinogen−base stacking conformations with the experimental NMR solution structures of this adduct at a primer−template junction (*30*) and in a duplex where the partner residue of the adducted guanine residue is missing (*29*). The extent of the dynamic mobility of the BP and G4 following the rearrangement is small, as shown by the small flexibility in the torsion angles α', β', and χ which govern the orientation of G4 and BP. The degree of flexibility is shown as polar plots in Figure 5, including the rearrangement.

Of course, a 225 ps molecular dynamics simulation only surveys the local potential energy surface of the system, and local equilibration is manifested in the relative stability of the α', β', and χ values following the rearrangement. In addition, another force field or another dynamics protocol could yield a different trajectory. Nonetheless, the structure that evolved in this simulation is a feasible one with some suggestive biological insight.

The rearrangement of the BP and concomitant local movement of the polymerase result in alteration of polymerase active site hydrogen bonding within the DNA minor groove. From the crystal structure of the β pol ternary complex, the side chains of residues Asn^{279}, Tyr^{271}, and Arg^{283} are within hydrogen bonding distance to the bases of the incoming deoxynucleoside 5′-triphosphate (i.e. ddCTP), the terminal primer nucleotide, and the templating guanine nucleotide, respectively (*11, 13*). These hydrogen bond donors are indiscriminate in that they bond to the O2 of pyrimidines or the N3 of purines in the DNA minor groove (*45*). In the computed structure, new hydrogen bonding interactions occur between Arg^{283} and Asn^{279} with O8 of the BP benzylic ring. Additionally, new hydrogen bond interactions are now observed between Arg^{283} and Asn^{279} and between the benzylic ring and G5. In contrast, the hydrogen bond between Tyr^{271} and the terminal primer base is lost during the simulation. Panels A and B of Figure 3 show key hydrogen bonding features of the starting structure and the representative 200 ps structure, respectively, and Table 1 summarizes hydrogen bond average distances and angles from the simulation. Watson−Crick hydrogen bonding between G5 and C18 is maintained throughout the simulation. Other stabilizing features in the structure maintained during the simulation following the initial rearrangement are favorable van der Waals interactions of alkyl portions of Lys^{280} and Asp^{276} with the aromatic pyrenyl moiety and favorable electrostatic interactions (salt bridge formation) between the charge centers of Lys^{280} and Asp^{276} (starting distance = 8.2 Å, average distance during the simulation = 5.8 Å, with a standard deviation of 0.9 Å). In the crystal structure of the β pol ternary complex, Asp^{276} makes van der Waals interactions with the base of the incoming ddCTP, and replacing this side chain with a smaller uncharged derivative results in enhanced binding (*46*). The Lys^{280} side chain was not visible in the electron density map of the rat ternary complex, but modeling suggests that it could easily interact with the templating guanine. Panels A and B of Figure 4 are space filling views of the starting structure and the structure at 200 ps, respectively.

Table 1: Hydrogen Bonding in Dynamics Simulation[a]

hydrogen bond	average distance (Å)	standard deviation (Å)	average angle (deg)	standard deviation (deg)
Arg^{283} NH···O8[BP]	3.0 (6.1)	0.3	145.8	18.4
Asn^{279} NH···O8[BP]	3.1 (6.1)	0.6	173.2	13.5
$G5N^2H$···O8[BP]	3.3 (4.0)	0.3	131.9	16.9
Arg^{283} NH···N[Asn^{279}]	3.7 (6.1)	0.5	175.5	8.6
Arg^{283} NH···O[Asn^{279}]	2.9 (4.9)	0.4	168.5	16.6

[a] Averaged over first 200 ps. Hydrogen bonds have begun to form by 3 ps. Values for starting structure are given in parentheses. Distances are from heavy atom to heavy atom.

A number of studies of the effects of the (+)-*trans-anti*-BP-N^2-dG adduct on DNA synthesis in vitro and in vivo have been carried out in recent years (*31*−*37*). These studies have shown that the base sequence context, the type of polymerase, and the type of cell system influence the results. However, two effects of the BP moiety are apparent in all systems: a predominant proclivity to cause polymerase blockage and, rarely, when the blockage is overcome, a tendency to cause G·A mismatches.

The structure we have obtained in the dynamics simulation with pol β could be expected to inhibit extension since entry of the incoming dNTP, which is hydrogen bonded to Asn^{279} in the crystal structure (*11*), would be impeded by the benzylic ring, which is now hydrogen bonded to Asn^{279}. Additionally, loss of this hydrogen bond interaction with the incoming deoxynucleoside 5′-triphosphate has been demonstrated to result in loss of binding free energy (*13, 47*). Most importantly, the BP moiety obstructs access to the Watson−Crick edge of the templating G4 to which it is attached. This templating G4 is shifted from its normal position and is no longer within hydrogen bonding distance to Arg^{283}, as in the crystal structure. This putative hydrogen bond between the guanidinium NH1 of Arg^{283} and N3 of the G4 template, together with stabilizing van der Waals interactions between

them, has been shown to be the key factor which governs both fidelity and catalytic efficiency (*13*). Instead, in the presence of the BP moiety, the Arg^{283} is hydrogen bonded to it, and the central role of Arg^{283} in correctly positioning and stabilizing the templating base for faithful and efficient nucleotide incorporation is compromised.

Alanine substitution for Arg^{283} has revealed not only a reduction in both fidelity and catalytic efficiency but also a strong tendency to induce G·A mispairing (*13*, *48*). These results are in line with the effects induced by the (+)-*trans-anti*-BP-N^2-dG adduct in DNA replication studies (*31*−*37*). Interaction of the critical Arg^{283} with the BP would inhibit its ability to position and stabilize the template for faithful and efficient extension, analogous to its substitution by alanine. For those rare cases where the BP-induced replication blockage is overcome by incorporation of adenine or another base, a conformational change would be required to make room for the incoming dNTP. Interestingly, a comparison of the α′, β′, and χ torsion angles in the present structure as shown in Figure 5 (average values of 206.2, 266.3, and 219.6°, respectively) with those in the experimental NMR solution structure (*28*) which placed the BP in the B-DNA minor groove with essentially intact Watson−Crick base pairing (α′, β′, and χ = 137, 258, and 257°, respectively) reveals that relatively modest torsional movements in α′ and χ would be needed to reorient the BP so that the G4 Watson−Crick edge would become accessible. Concomitant rearrangement of the enzyme would have to accompany this motion, as well as some torsional shifts in the DNA backbone. The C-terminal domain of β pol, residues 260−335, is known to be conformationally flexible (*12*, *13*).

The NMR solution structure of this BP adduct at a primer−template junction in a different sequence context and without enzyme (*30*) also manifests displacement of the modified guanine with stacking of the BP with the adjacent base pair. However, the α′, β′, and χ values (272, 201, and 71°, respectively) in a representative conformer (*26*) from this ensemble reveal a major distinction in the glycosidic torsion angle χ, which is in the abnormal syn domain in the solution structure while it is in the normal anti domain in the structure with polymerase that evolved in the present simulation. In the NMR solution structure, the syn modified and displaced deoxyguanosine residue is extended to accommodate the BP. This minimizes the BP's exposure to solvent as it interacts with the adjacent base pair on one face, and with its attached guanine and other residues in the single-stranded portion of the template on the other face. In the present computed structure, interactions with the enzyme play an important part in satisfying the hydrophobic character of the BP.

Replication blockage by a bulky adduct can readily be envisioned to result from any number of conformers that impede access to the damaged template. While DNA replication studies past this BP lesion have not yet been carried out with pol β, blockage is a likely effect, in line with observations with other polymerases. Possible analogies between β pol and other replicating enzymes suggest the possibility that a specific blocking conformation, such as the one that evolved in our simulation, could be stabilized by interactions of the BP with amino acid residues of the polymerase that are essential for efficient and faithful extension. The crystal structure of *Taq* polymerase with double-stranded DNA is consistent with the idea that critical interactions (i.e. DNA minor groove hydrogen bonding) are conserved between different families of polymerases (*49*).

REFERENCES

1. Wiebauer, K., and Jiricny, J. (1990) *Proc. Natl. Acad. Sci. U.S.A. 87*, 5842−5845.
2. Dianov, G., and Lindahl, T. (1994) *Curr. Biol. 4*, 1069−1076.
3. Horton, J. K., Srivastava, D. K., Zmudzka, B. Z., and Wilson, S. H. (1995) *Nucleic Acids Res. 23*, 3810−3815.
4. Singhal, R. K., Prasad, R., and Wilson, S. H. (1995) *J. Biol. Chem. 270*, 949−957.
5. Sobol, R. W., Horton, J. K., Huhn, R., Gu, H., Singhal, R. K., Prasad, R., Rajewsky, K., and Wilson, S. H. (1996) *Nature 379*, 183−186.
6. Klungland, A., and Lindahl, T. (1997) *EMBO J. 16*, 3341−3348.
7. Linn, S. (1991) *Cell 66*, 185−187.
8. Jenkins, T. M., Saxena, J. K., Kumar, A., Wilson, S. H., and Ackerman, E. J. (1992) *Science 258*, 475−478.
9. Sweasy, J. B., and Loeb, L. A. (1992) *J. Biol. Chem. 267*, 1407−1410.
10. Wilson, S. H. (1990) in *The Eukaryotic Nucleus: Molecular Biochemistry and Macromolecular Assemblies* (Strauss, P. R., and Wilson, S. H., Eds.) Vol. 1, pp 199−233, Telford Press, Inc., Caldwell, NJ.
11. Pelletier, H., Sawaya, M. R., Kumar, A., Wilson, S. H., and Kraut, J. (1994) *Science 264*, 1891−1903.
12. Pelletier, H., Sawaya, M. R., Wolfle, W., Wilson, S. H., and Kraut, J. (1996) *Biochemistry 35*, 12742−12761.
13. Beard, W. A., Osheroff, W. P., Prasad, R., Sawaya, M. R., Jaju, M., Wood, T. G., Kraut, J., Kunkel, T. A., and Wilson, S. H. (1996) *J. Biol. Chem. 271*, 12141−12144.
14. Harvey, R. G. (1991) *Polycyclic Aromatic Hydrocarbons: Chemistry and Carcinogenicity*, Cambridge University Press, Cambridge, England.
15. Grimmer, G. (1993) in *Proceedings of the 13th International Symposium on Polynuclear Aromatic Hydrocarbons* (Garrigues, P., and Lamotte, M., Eds.) pp 31−41, Gordon and Breach Science Publishers, Langhorne, PA.
16. Perrin, J. L., Poirot, N., Liska, P., Hanras, C., Theinpont, A., and Felix, G. (1993) in *Proceedings of the 13th International Symposium on Polynuclear Aromatic Hydrocarbons* (Garrigues, P., and Lamotte, M., Eds.) pp 337−346, Gordon and Breach Science Publishers, Langhorne, PA.
17. Buening, M. K., Wislocki, P. G., Levin, W., Yagi, H., Thakker, D. R., Akagi, H., Koreeda, M., Jerina, D. M., and Conney, A. H. (1978) *Proc. Natl. Acad. Sci. U.S.A. 75*, 5358−5361.
18. Slaga, T. J., Bracken, W. J., Gleason, G., Levin, W., Yagi, H., Jerina, D. M., and Conney, A. H. (1979) *Cancer Res. 39*, 67−71.
19. Weinstein, I. B., Jeffrey, A. M., Jennette, K. W., Blobstein, S. H., Harvey, R. G., Harris, C., Autrup, H., Kasai, H., and Nakanishi, K. (1976) *Science 193*, 592−594.
20. Jeffrey, A. M., Jennette, K. W., Blobstein, S. H., Weinstein, I. B., Beland, F. A., Harvey, R. G., Kasai, H., Miura, I., and Nakanishi, K. (1976) *J. Am. Chem. Soc. 98*, 5714−5715.
21. Osborne, M. R., Beland, F. A., Harvey, R. G., and Brookes, P. (1976) *Int. J. Cancer 18*, 362−368.
22. Cheng, S. C., Hilton, B. D., Roman, J. M., and Dipple, A. (1989) *Chem. Res. Toxicol. 2*, 334−340.
23. Sayer, J. M., Chadha, A., Agarwal, H. S. K., Yeh, H. J. C., Yagi, H., and Jerina, D. M. (1991) *J. Org. Chem. 56*, 20−29.
24. Denissenko, M. F., Pao, A., Tang, M., and Pfeifer, G. (1996) *Science 274*, 430−432.
25. Harris, C. C. (1993) *Science 262*, 1980−1981.
26. Geacintov, N. E., Cosman, M., Hingerty, B. E., Amin, S., Broyde, S., and Patel, D. J. (1997) *Chem. Res. Toxicol. 10*, 111−146.
27. Singh, S. B., Hingerty, B. E., Singh, U. C., Greenberg, J. P., Geacintov, N. E., and Broyde, S. (1991) *Cancer Res. 51*, 3482−3492.

28. Cosman, M., de los Santos, C., Fiala, R., Hingerty, B. E., Singh, S. B., Ibanez, V., Margulis, L. A., Live, D., Geacintov, N. E., Broyde, S., and Patel, D. J. (1992) *Proc. Natl. Acad. Sci. U.S.A. 89*, 1914−1918.
29. Cosman, M., Fiala, R., Hingerty, B. E., Amin, S., Geacintov, N. E., Broyde, S., and Patel, D. J. (1994) *Biochemistry 33*, 11507−11517.
30. Cosman, M., Hingerty, B. E., Geacintov, N. E., Broyde, S., and Patel, D. J. (1995) *Biochemistry 34*, 15334−15350.
31. Mackay, W., Benasutti, M., Drouin, E., and Loechler, E. L. (1992) *Carcinogenesis 13*, 1415−1425.
32. Hruszkewycz, A. M., Canella, K. A., Peltonen, K., Kotrappa, L., and Dipple, A. (1992) *Carcinogenesis 13*, 2347−2352.
33. Rodriguez, H., and Loechler, E. L. (1993) *Carcinogenesis 14*, 373−383.
34. Shibutani, S., Margulis, L. A., Geacintov, N. E., and Grollman, A. P. (1993) *Biochemistry 32*, 7531−7541.
35. Jelinsky, S. A., Liu, T., Geacintov, N. E., and Loechler, E. L. (1995) *Biochemistry 34*, 13545−13553.
36. Moriya, M., Spiegel, S., Fernandes, A., Amin, S., Liu, T.-M., Geacintov, N. E., and Grollman, A. P. (1996) *Biochemistry 35*, 16646−16651.
37. Hanrahan, C. J., Bacolod, M. D., Vyas, R. R., Liu, T., Geacintov, N. E., Loechler, E. L., and Basu, A. K. (1997) *Chem. Res. Toxicol. 10*, 369−377.
38. Dunbrack, R. L., and Karplus, M. (1993) *J. Mol. Biol. 230*, 543−574.
39. Arnott, S., and Hukins, D. W. L. (1973) *J. Mol. Biol. 81*, 93−105.
40. Pearlman, D., Case, D., Caldwell, J., Seibel, G., Singh, U. C., Weiner, P., and Kollman, P. A. (1986, 1991) *AMBER 4.0 Documentation*, University of California, Berkeley, CA.
41. Cornell, W. D., Cieplak, P., Bayly, C. I., Gould, I. R., Merz, K. M., Ferguson, D. M., Spellmeyer, D. C., Fox, T., Caldwell, J. W., and Kollman, P. A. (1995) *J. Am. Chem. Soc. 117*, 5179−5197.
42. Jorgenson, W. L., Chandrasekhar, J., Madura, J. D., Impey, R. W., and Klein, M. L. (1983) *J. Chem. Phys. 79*, 926−935.
43. van Gunsteren, W. F., and Berendsen, H. J. C. (1977) *Mol. Phys. 34*, 1311−1327.
44. McCammon, J. A., and Harvey, S. (1987) *Dynamics of Proteins and Nucleic Acids*, Cambridge University Press, Cambridge, England.
45. Seeman, N. C., Rosenberg, J. M., and Rich, A. (1976) *Proc. Natl. Acad. Sci. U.S.A. 73*, 804−808.
46. Lavrik, O. I., Prasad, R., Beard, W. A., Safronov, I. V., Dobrikov, M. I., Srivastava, D. K., Shishkin, G. V., Wood, T. G., and Wilson, S. H. (1996) *J. Biol. Chem. 271*, 21891−21897.
47. Kraynov, V. S., Werneburg, B. G., Zhong, X. J., Lee, H., Ahn, J. W., and Tsai, M. D. (1997) *Biochem. J. 323*, 103−111.
48. Ahn, J., Werneburg, B. G., and Tsai, M. D. (1997) *Biochemistry 36*, 1100−1107.
49. Eom, S. H., Wang, J. M., and Steitz, T. A. (1996) *Nature 382*, 278−281.

BI9720639